HHS Public Access

Author manuscript

Cancer Gene Ther. Author manuscript; available in PMC 2011 August 01.

Published in final edited form as:

Cancer Gene Ther. 2011 February ; 18(2): 135–143. doi:10.1038/cgt.2010.64.

ROLE OF RAC-1 DEPENDENT NADPH OXIDASE IN THE GROWTH OF PANCREATIC CANCER

Juan Du, **Jingru Liu**, **Brian J. Smith**, **Ming-Sound Tsao**, and **Joseph J. Cullen**

Departments of Surgery (JJC), Radiation Oncology (JL, JD, JJC), University of Iowa College of Medicine, Iowa City, IA, and the Holden Comprehensive Cancer Center (BJS, JJC), and Veterans Affairs Medical Center (JJC), Iowa City, IA. and the Department of Pathology and Division of Cellular Molecular Biology and the Ontario Cancer Institute/Princess Margaret Hospital Toronto, and University of Toronto, Ontario, Canada (MST)

Abstract

K-*ras* mutations occur in as high as 95% of patients with pancreatic cancer. K-*ras* activates Rac1-dependent NADPH oxidase, a key source of superoxide. Superoxide plays an important role in pancreatic cancer cell proliferation and scavenging or decreasing the levels of superoxide inhibits pancreatic cancer cell growth both *in vitro* and *in vivo.* DNA microarray analysis and RT-PCR has demonstrated that Rac1 is also upregulated in pancreatic cancer. The aim of this study was to determine if inhibiting Rac1 would alter pancreatic tumor cell behavior. Human pancreatic cancer cells with mutant K-*ras* (MIA PaCa-2), wild-type K-*ras* (BxPC-3), and the immortal H6c7 cell line (pancreatic ductal epithelium) expressing K-*ras* oncogene (H6c7eR-K*ras*T) that is tumorigenic, were infected with a dominant/negative Rac1 construct (Ad*N17Rac1)*. In cells with mutant K-*ras,* Ad*N17Rac1* decreased rac activity, decreased superoxide levels, and inhibited *in vitro* growth. However in the BxPC-3 cell line, Ad*N17Rac1* did not change rac activity, superoxide levels, or *in vitro* cell growth. Additionally, Ad*N17Rac1* decreased superoxide levels and inhibited *in vitro* growth in the KrasT tumorigenic cell line, but had no effect in the immortalized H6c7 cell line. In human pancreatic tumor xenografts, intratumoral injections of Ad*N17Rac1* inhibited tumor growth. These results suggest that activation of Rac1-dependent superoxide generation leads to pancreatic cancer cell proliferation. In pancreatic cancer inhibition of Rac1 may be a potential therapeutic target.

Keywords

Rac-1; NADPH oxidase; pancreatic cancer; reactive oxygen species

Address correspondence to Joseph J. Cullen, M.D., 4605 JCP, 200 Hawkins Drive, University of Iowa Hospitals and Clinics, Iowa City, IA 52242. joseph-cullen@uiowa.edu W: (319) 353-8297, Fax: (319) 356-8378.
Jingru Liu and Juan Du contributed equally to this work.

Conflict of Interest

There are no financial or other interests with regard to the submitted manuscript that might be construed as a conflict of interest.

INTRODUCTION

K-*ras* mutation results in constitutive activation of intracellular signaling pathways, leading to uncontrolled cellular proliferation. Mutations of the K-*ras* gene occur in 95% of cases with adenocarcinoma of the pancreas (1). Although mutations of K-*ras* are less common in other cancer types, K-*ras* mutation has been found in intraductal pancreatic cancer, ductal hyperplasia, and even chronic pancreatitis (2), suggesting that this may be an early event in pancreatic carcinogenesis. Although the entire spectrum of downstream genes regulated by the K-*ras* activation is not clear, several Ras-mediated signaling pathways and their target proteins have been demonstrated to regulate pancreatic cancer growth and survival. Multiple lines of evidence demonstrate that downstream proteins, such as the G proteins Rac and Rho, are upregulated in pancreatic cancer, and K-*ras* activated Raf-1 and Rac more effectively than the other *ras* isoforms, Ha-*ras* and N-*ras* (3). Further understanding of these key molecular events in pancreatic carcinogenesis has provided a potential target for novel gene therapies.

Rac may represent an important downstream effecter for Ras activation in many cells (4). In fact, DNA microarray analysis and RT-PCR has demonstrated that Rac1 is also upregulated in pancreatic cancer (5). Rac, a member of the Rho family, is a 21-kDa GTP binding protein. The rho activation cycle regulated by GDP exchange factors and GTPase activating factors catalyze the exchange of inactive GDP bound form to an active GTP bound form (6). There are three isoforms of Rac; Rac1 expression is ubiquitous, but Rac2 is expressed only in hematopoietic cells (7). Rac3 is highly expressed in the brain but in lower levels in a variety of other tissues (8).

Two major functions of Rac1 have been identified including regulation of the organization of the actin cytoskeleton; the other one is controlling the activity of the key enzyme complex NADPH oxidase to mediatesuperoxide production (9). Several groups have reported that Rac1 activation of NADPH oxidase occurs not only in phagocytes, but also in nonphagocytes (10). The subunit composition of the NADPH oxidase complex in the phagocytic cell consists of a plasma membrane flavocytochrome, cytochrome b558, comprised of two subunits gp91phox and p22phox, with additional cytoplasmic components p47phox, p67phox and the Rac1 (3). The NADPH-driven reduction of oxygen to $O_2^{\bullet -}$ requires FAD as a cofactor.

The contribution of Rac proteins to the activation of the phagocyte NADPH oxidase has been studied extensively and has recently seen important progress in the analysis in mouse models (11). Several studies have subsequently implicated Rac1-mediated production of reactive oxygen species (ROS) in a variety of cellular responses. Studies by Irani *et al.*, have shown that superoxide production in NIH 3T3 (fibroblastic clonal lines) transformed cells was dependent upon farnesylation of Ras, required Rac1 activity, and the activity of NADPH oxidase complex (12). Using an activated mutant of Rac1, V12Rac1, resulting in increased production of ROS in fibroblasts, Sundaresan has shown the direct link between Rac1 activity and ROS production in nonphagocytic cells (13). Wetering and Moldovan suggested that the constitutive active form of Rac1 increased the production of ROS in endothelial cells, and induced loss of cell–cell adhesion and cytoskeletal reorganization (14,

15). Rac1-mediated production of ROS was also found in HeLa cells and implicated in IL-1ß– mediated activation of NF-κB, further strengthening the idea that Rac1-mediated production of intracellular ROS is instrumental in signal transduction (16). Other studies have shown that downregulation of Rac1 activity by using dominant negative Rac1 mutant, N17Rac1, suppressed NADPH oxidase activity and decreased superoxide production (17). In addition, based on expression of N17Rac1 and the use of the antioxidants, activation of protein tyrosine phosphorylation and extracellular-signal regulated kinase is a Rac1- and ROS-dependent manner (18). Various mechanisms of the Rac1-induced ROS have been proposed. Deem and Cook-Mills suggested that endothelial NADPH oxidase 2 (NOX2) releases ROS extracellularly and stimulates matrix metalloprotease activity (19). Most importantly in pancreatic cancer, Rac activation increases the invasive capacity of pancreatic cancer through NADPH oxidase ROS production (20). Taken together, there is ample evidence for Rac-dependent production of ROS by the NADPH oxidase complex in cellular signaling.

Our present study demonstrates that inhibition of Rac1 activity by using a dominant/ negative Rac1 mutant construct inhibited growth in human pancreatic cancer cells with mutant K-*ras* and in tumorigenic immortalized pancreatic ductal epithelial cells, but not in pancreatic cancer cells with wild-type K-ras or in immortalized pancreatic ductal epithelial cells (non-tumorigenic). The growth inhibitions correlated with decreased steady-state levels of superoxide. Since 95% of pancreatic cancers express mutant K-*ras*, inhibition of Rac1 may be a potential therapeutic target.

MATERIALS AND METHODS

Cell culture

The following human pancreatic adenocarcinoma cell lines were obtained from American Type Culture Collection (Rockville, MD): BxPC-3 (poorly differentiated, wild-type *K-ras*), and MIA PaCa-2 (undifferentiated, mutant *K-ras*). BxPC-3 was maintained in RPMI 1640 with 10% fetal bovine serum. MIAPaCa-2 was maintained in Dulbecco modified Eagle medium supplemented with 10% fetal bovine serum and 2.5% horse serum. All media was obtained from Invitrogen (Carlsbad, CA) and all cell lines were maintained at 37°C in 5% CO_2/95% air. In addition, we used an immortalized pancreatic ductal epithelial cell line with near normal genotype and phenotype of pancreatic duct epithelial cells HPV16-E6E7 (H6c7), and the isogenic cell line that expresses K-*ras*^{G12V} and forms tumors H6c7eR-KrasT (21). These cell lines were maintained in keratinocyte serum free media and supplemented with epidermal growth factor and bovine pituitary extract as previously described (22). Initial work with these cells demonstrated that they did not form colonies. Thus, feeder cells were used and prepared by growing B1 mouse fibroblast cells in DMEM containing 10% FBS and 1% penicillin and streptomycin plus 1x MEM with nonessential amino acids. Cells were then plated in 100-mm dishes and grown to 80% confluence before being irradiated for 37.61 min for a total dose of 30 Gy. The cells were harvest and preserved in growth media containing 10% DMSO and aliquots were frozen in liquid nitrogen. Twenty-four hours before clonogenic assay, irradiated cells were thawed and

diluted in keratinocyte serum free media. Cells were then seeded 3×10^5 per well in 6-well plates as described (23).

Adenovirus Gene Transfer

Ad*N17Rac1-HA* (Ad*N17Rac1*) is a "first-generation" adenoviral vector (E1 deleted/E3 partially deleted) encoding HA-epitope tagged cDNA of dominant/negative N17Rac1 containing a substitution at position 17 and was obtained from the University of Iowa Gene Transfer Vector Core. The promoter is a human cytomegalovirus (hCMV) promoter. The Ad*N17Rac1* was constructed by PCR amplification of cDNA sequences using primers that incorporated an N-terminal HA fusion to Rac1 (17). Approximately 10^6 MIA PaCa-2 cells were plated in 5 ml of complete media in a 100-mm^2 plastic dish and allowed to attach for 24 hours. Cells were then washed three times in serum-and antibiotic-free media. The Ad*N17Rac1* suspended in 3% sucrose-PBS, was then applied to cells suspended in 5 ml of antibiotic-free media at 0, 10, 25, 50, and 100 MOI (multiplicity of infection). Control cells were treated with 100 MOI of the Ad*BglII* or Ad*Empty* constructs. Ad*BglII* only has the adenovirus cassette; it does not have any promoter or poly A sequence. The Ad*Empty* vector has the adenovirus cassette plus the promoter sequence but no transgene. Cells were incubated with the adenovirus constructs for 24 hours. Media was then replaced with 5 ml of complete media.

Cell Homogenization and Protein Determination

Cells were removedfrom the dish using a plastic scraper after washing three times in PBS (pH 7.0), and then suspended in potassium phosphatebuffer (pH 7.8). The cell pellets were sonicated on icethree times for 10 s each using a VibraCell sonicator (Sonicsand Materials Inc., Danbury, CT) at 30% duty cycle. Total protein concentrations were determined using the Bio-Rad (BioRad, Hercules, CA)protein assay kit according to the manufacturer's instruction.

Immunoblot Analysis

Immunoreactive protein corresponding to Rac1 was identified and quantitated from total cell protein by the specific reaction of the immobilized protein with its antibody. Total protein was electrophoresed in a 12.5% SDS-polyacrylamide running gel and a 5% stacking gel. The proteins were then electotransferred to nitrocellulose sheets. After transfer, the membranes were blocked in 5% nonfat dry milk in TTBS (10 mM Tris-HCl, 150 mM NaCl (pH 8.0), 0.05% Tween 20) at room temperaturefor 1 h. To detect specific proteins, the membrane was incubated with specific antibody. After incubation overnight in 1:1000 dilution of primary antibody to Rac1, MnSOD or CuZnSOD (Cell Signalling Technology, Danvers, MA) at 4 C, membranes are incubated with goat anti-mouse IgG or goat anti-rabbit (1:10 000, Chemicon International, Temecula, CA) at room temperature for 1 h. The washed blot was then treated with SuperSignal West Pico Chemiluminescent substrate (Pierce Biotechnology, Rockford, IL) and exposed to Classic Blue Autoradiography Film (MIDSCI^{TM}, St. Louis, MO). Western blots were performed in duplicate. β-actin was used to determine equal loading.

Cell Growth

Cells (1×10^4) were plated in 3 ml complete media in 6-well plates. Cells were trypsinized and then counted everyday for a week using a Coulter counter. Cell population doubling time in hours (*DT*) was determined using the following equation: *DT* (hours) = $0.693(t - t_o)/\ln (N_t/N_o)$ where t_o = time at which exponential growth began, t = time in hours, N_t = cell number at time t, and N_o = initial cell number. For controls the Ad*BglII* or Ad*Empty* vector constructs were given to equal the viral load of the dominant/negative rac viral construct.

Plating Efficiency

Cells were infected with the Ad*N17Rac*, Ad*BglII*, or Ad*Empty* vectors and were plated into 6-well plates in complete media. The dishes were maintained in the incubator for 14 days to allow colony formation. The colonies were then fixed and stained with 0.1% crystal violet and 2.1% citric acid, and those colonies containing greater than 50 cells were scored.

Measurement of superoxide

Intracellular levels of superoxide were detected using the oxidant-sensitive probe hydroethidine (Invitrogen, Carlsbad CA). The oxidation products of hydroethidine bind to DNA in the nucleus and give a red fluorescence when oxidized by $O_2^{\bullet -}$. Cells were grown in 60 mm plates and incubated with different treatments as described previously.Forty-eight hours later, the cells were washed and incubatedfor 45 minutes with hydroethidine (10 μM) in HBSS at 37 °C and after incubation the cells were rinsed, cells were collected into Eppendorf tubes, cell pellets were lysed by 1% NP-40. After centrifugation, supernatant were transferred to a 96-well black bottom plate. The intensity of fluorescence (excitation 485 nm, emission 595 nm) was measured using a Tecan Spectra Fluor Plus microplate reader (Tecan, Research Triangle Park, NC). The relative fluorescence intensity wascalculated by dividing the total fluorescence intensity by total protein.

Rac1 activation assay

Rac1 activity was measured in pancreatic cancer cells using a Rac1 activation assay kit (Upstate Biotechnology, Temecula, CA). Cells that were approximately 80% confluent were washed twice with ice-cold PBS and lysed in ice-cold MLB (25 mM HEPES, 150 mM NaCl, 1% Igepal CA-630, 10 mM $MgCl_2$, 1 mM EDTA and 2% glycerol). Cell lysate were centrifuged at 14000 × g for 5 min at 4 °C. Supernatant containing the same amount of protein was incubated with PAK1-PBD agarose for 1 h at 4 °C. Active (GTP-bound) Rac binds specially to the p21-binding domain of p21-activated protein kinase 1. Precipitated GST bound Rac1 were resolved on a 4–20% Tris-HCl Ready Gel (Bio-Rad, Hercules, CA) and immunoblotted using anti-Rac1monoclonal antibody (1:1000, Upstate Biotechnology).

Adenovirus Vector-Mediated *N17Rac1 in vivo* Gene Transfer

Thirty-day-old athymic nude mice (Nu/NU) were obtained from Harlan Sprague-Dawley (Indianapolis, IN). The nude mice protocol was reviewed and approved by the Animal Care and Use Committee of the University of Iowa and were in compliance with The U.S. Public Health Service *Policy on Humane Care and Use of Laboratory Animals (NIH).* The animals were housed four to a cage and fed a sterile commercial stock diet and tap water, *ad libitum*.

Animals were allowed to acclimate in the unit for one week before any manipulations were performed. MIA PaCa-2 tumor cells (3×10^6) were delivered subcutaneously into the flank region of the mice with a 1-cc tuberculin syringe equipped with a 25-gauge needle. The tumors were allowed to grow until they reached between 3 mm and 4 mm in greatest dimension (2 weeks), at which time they were treated with adenovirus. The adenovirus constructs were delivered through two injection sites in the tumor. Approximately 1×10^9 plaque-forming units (PFU) in 50 μL of PBS of the Ad*N17Rac1* constructs were delivered to the tumor by means of a 25-gauge needle attached to a 1-cc tuberculin syringe on days 1, 7, and 14 for a total of 3 injections. Control tumors received PBS, or adenovirus containing no gene (Ad*Empty*) in similar volumes and PFUs at the same time points. There were 7–8 mice in each treatment group. Tumor size was measured every two to three days by means of a vernier caliper, and tumor volume was estimated according to the following formula: tumor volume = $\pi/6 \times L \times W^2$, where L is the greatest dimension of the tumor, and W is the dimension of the tumor in the perpendicular direction (24). Animals were killed by CO_2 asphyxiation when the tumors reached a predetermined size of 1000 mm^3 and this was considered the time to sacrifice.

Statistical Analysis

Statistical analysis for the *in vitro* studies was performed using SYSTAT. A single factor ANOVA, followed by post-hoc Tukey test, was used to determine statistical differences between means. All means were calculated from three experiments, and error bars represent standard error of the mean (SEM). All western blots, activity assays, and activity gel assays were repeated at least twice. For the *in vivo* studies, the statistical analyses focused on the effects of different treatments on cancer progression. The primary outcome of interest was tumor growth over time. Once tumors were visible, the mice were then randomly assigned to a treatment group and followed until death or until the experiment was terminated. Tumor sizes (mm^3) were measured throughout the experiments, resulting in repeated measurements across time for each mouse. Linear mixed effects regression models were used to estimate and compare the group-specific tumor growth curves. In the growth curve analyses, statistically significant global tests of equality across groups were followed up with pairwise comparisons to identify specific group differences. All tests were two-sided and carried out at the 5% level of significance. Analyses were performed with the SAS and R statistical software packages.

RESULTS

Infection of mutant K-ras pancreatic cancer cells with AdN17Rac1 increases Rac1 protein, decreases Rac1 activity, and inhibits growth

MIA PaCa-2 cells that express mutant K-*ras* were transduced with Ad*N17Rac1* and showed a dose-dependent increase in expression of the N17 Rac1 immunoreactivity at 48 h after the infection with the adenovirus (Figure 1A). To ensure equal proteinloading, actin expression was measured. There is a significant increase in Rac1 immunoreactive protein with 25 MOI of Ad*N17Rac1* when compared to cells treated with the Ad*BglII* (100 MOI) vector. The maximum increase in Rac1 immunoreactive protein appears to occur at 100 MOI of the Ad*N17Rac1* vector. In contrast, Rac activity decreased with increasing N17 Rac1

immunoreactivity (Figure 1B). The Rac-GTP binding assay demonstrated that rac activity decreased with increasing viral titer. The maximum decrease in rac activity was seen with 100 MOI of the Ad*N17Rac1* vector. The increase in Rac1 immunoreactivity and decrease in rac activity inhibited cell growth. Figure 1C demonstrates significant inhibition of cell growth after infection of MIA PaCa-2 cells with 25, 50, and 100 MOI of the Ad*N17Rac1* vector. At day 6, cell number decreased by 73% with the 100 MOI Ad*N17 Rac1*compared with Ad*BglII* 100 MOI. In addition, cell doubling time increased significantly. Cell doubling time in controls and cells infected with the Ad*BglII* vector were 22 ± 1 and 22 ± 1 hour, respectively. Infection with the Ad*N17Rac1* vector significantly increased doubling time to 25 ± 1* with 25 MOI, 27 ± 2* with 50 MOI and 32 ± 2* hours with 100 MOI (n =3, *P < 0.05 vs. Ad*BglII*, Means ± SEM).

Next, we tested the ability of the Ad*N17Rac1*-transduced MIA PaCa-2 cells to form colonies. Plating efficiency also decreased with infection of the Ad*N17Rac1* vector. Figure 1D. Plating efficiency decreased by 47% with infection of 100 MOI of the Ad*N17Rac1* vector compared to infection with 100 MOI Ad*BglII* (n =3, P < 0.05 vs. Ad*BglII*, Means ± SEM). Thus, infection of mutant K-*ras* pancreatic cancer cells with a dominant/negative rac construct increased rac1 immunoreactive protein, decreased rac activity and inhibited *in vitro* cell growth characteristics.

Infection of wild-type K-ras pancreatic cancer cells with AdN17Rac1 increases immunoreactive protein but does not inhibit rac activity and does not affect growth

BxPC-3 cells that express wild-type K-*ras* were transduced with Ad*N17Rac1* and showed a dose-dependent increase in expression of the N17 Rac1 immunoreactivity at 48 h after the infection with the adenovirus (Figure 2A). There was a significant increase in Rac1 immunoreactive protein with 25 MOI of Ad*N17Rac1* when compared to cells treated with the Ad*BglII* (100 MOI) vector. The maximum increase in Rac1 immunoreactive protein appeared to occur at 100 MOI of the Ad*N17Rac1* vector. Unlike the MIA PaCa-2 cells that express mutant K-*ras*, the increase in Rac1 immunoreactivity did not affect cell growth in the BxPC-3 cell line. Figure 2B demonstrates no changes in cell growth after infection of BxPC-3 cells with 25, 50, and 100 MOI of the Ad*N17Rac1* vector. In addition, cell doubling time did not change. Cell doubling time in controls and cells infected with the Ad*BglII* vector were 52 ± 1 and 52 ± 2 hours, respectively. Infection with the Ad*N17Rac1* vector changed little with doubling times of 53 ± 1 with 25 MOI, 53 ± 2 with 50 MOI and 53 ± 2 with 100 MOI (n = 3, P > 0.05 vs. Ad*BglII*, Means ± SEM).

Next, we tested the ability of the Ad*N17Rac1*-transduced BxPC-3 cells to form colonies. Once again, infection with the Ad*N17Rac1* vector increased immunoreactive protein (Figure 2C). However, unlike the MIA PaCa-2 cells, the BxPC-3 cells infected with Ad*N17Rac1* 100 MOI had little change in Rac1 activity (Figure 2C). There were no significant changes in plating efficiency with infection of the Ad*N17Rac1* vector (Figure 2D) when compared to infection with 100 MOI Ad*BglII*. Thus, infection of wild-type K-*ras* pancreatic cancer cells with a dominant/negative rac construct increased rac1 immunoreactive protein, but did not change rac activity or *in vitro* cell growth characteristics.

Superoxide levels decreased in MIA PaCa-2 cells after infection with the AdN17Rac1 construct without changes in antioxidant proteins that scavenge superoxide

One of the major functions of Rac1 includes controlling the activity of NADPH oxidase to mediate superoxide production (14). Intracellular levels of superoxide were detected following infection of the MIA PaCa-2 and BxPC-3 cell lines with Ad*N17Rac1*. As a positive control, we also used Ad*MnSOD* and DPI, a non-specific inhibitor of flavin oxidases like NADPH oxidase. Ad*N17 Rac1* (100 MOI) decreased hydroethidine fluorescence by 18% ± 2 in MIA PaCa-2 cells when compared to the same cells treated with the Ad*BglII* vector (100 MOI) (Figure 2E). In addition, treatment of cells with Ad*MnSOD* (100 MOI) also decreased hydroethidine fluorescence 14% ± 5, while DPI 15 μM decreased hydroethidine fluorescence by 32% ± 6 (data not shown, means ± SEM, n = 3, $P < 0.05$ vs Ad*BglII*). Hydroethidine fluorescence did not change significantly when BxPC-3 cells were infected with Ad*N17Rac1* 100 MOI when compared to the same cells infected with the Ad*BglII* vector (Figure 2E). Next we wanted to determine if the change in hydroethidine fluorescence was mediated by Rac1 inhibition, and not increases in either CuZnSOD or MnSOD, the two superoxide dismutase enzymes that scavenge superoxide. Western blots for MnSOD and CuZnSOD demonstrated no change in immunoreactive protein in MIA PaCa-2 cells infected with the Ad*N17Rac1* construct (25–100 MOI) when compared to the parental cell line or cells infected with the Ad*BglII* vector (Figure 2F).

Infection of immortalized H6c7 cell line with AdN17Rac1 has no effect on growth, while infection of the isogenic cell line that expresses K-ras with AdN17Rac1 increases Rac1 protein and inhibits growth

To further characterize the mechanism of Rac1 activity in the growth of pancreatic cancer, we used an immortalized pancreatic ductal epithelial cell line with near normal genotype and phenotype of pancreatic duct epithelial cells HPV16-E6E7 (H6c7), and the isogenic cell line that expresses K-*ras*^{G12V} and forms tumors H6c7eR-KrasT (KrasT) (21). Infection of these cell lines with the Ad*N17Rac* vector (100 MOI) demonstrated increased immunoreactive protein when compared to the parental cell lines and cells infected with the Ad*Empty* vector (100 MOI) (Figure 3A). We then tested the ability of these cells to form colonies after infection with the Ad*N17Rac1* vector. In the H6c7 cell lines, infection with Ad*N17Rac1* 100 MOI did not change plating efficiency when compared to infection with 100 MOI Ad*Empty* (means ± SEM, n = 3, $P > 0.05$ vs. Ad*Empty*). (Figure 3B). However, infection with 100 MOI Ad*N17Rac1* significantly decreased plating efficiency in the KrasT cells (means ± SEM, n = 3, $P < 0.05$ vs. Ad*Empty*). (Figure 3B). Thus, infection of immortalized pancreatic ductal epithelial cells with a dominant/negative rac construct increased rac1 immunoreactive protein, but did not significantly change *in vitro* cell growth characteristics. However, infection of the isogeneic cell line that expresses K-*ras* with a dominant/negative rac construct also increased rac1 protein and inhibited cell growth.

Next we also measured hydroethidine fluorescence in the H6c7 and KrasT cells. Forty-eight hours after infection with Ad*Empty* or Ad*N17Rac1* vectors, H6c7 and KrasT cells were incubatedfor 45 minutes with hydroethidine (10 μM) and the intensity of fluorescence was measured using flow cytometry. Ad*N17 Rac1* (100 MOI) decreased hydroethidine fluorescence by 40% ± 6 in KrasT cells when compared to the same cells treated with the

Ad*Empty* vector (100 MOI) (Figure 3C). In contrast, hydroethidine fluorescence did not change significantly when H6c7 cells were infected with Ad*N17 Rac1* 100 MOI when compared to the same cells infected with the Ad*Empty* vector (Figure 3C). As seen in the other pancreatic cancer cell lines, Western blots for MnSOD and CuZnSOD demonstrated no change in immunoreactive protein in the KrasT cells infected with the Ad*N17Rac1* construct (100 MOI) when compared to the parental cell line or cells infected with the Ad*Empty* vector (Figure 3D).

Ad*N17Rac1* decreases in vivo tumor growth

To determine if Ad*N17Rac1* could reduce tumor growth *in vivo*, the Ad*N17Rac1* or Ad*Empty* constructs were delivered to pre-established tumors (3– 4 mm) on days 1, 7, and 14 for a total of 3 injections. On day 1 when the adenoviral injections were started the mean tumor volume in the controls was 47 ± 10, 76 ± 25 in the Ad*Empty* group and 47 ± 9 in the AdN17 Rac1 group (Means ± SEM, $P > 0.05$ between groups). When the Ad*N17Rac1* construct was given, a slower growth in tumor was observed in comparison to the control group as well as the Ad*Empty* injected group as seen in the estimated growth curves in Figure 4. For example, on Day 17, the control and the Ad*Empty* group had mean tumor volumes of 745 mm^3 and 582 mm^3, respectively, while the Ad*N17Rac1* group had a mean tumor volume of 47 mm^3 ($P = 0.001$ vs Ad*Empty*, n = 7 – 8 mice/group).

DISCUSSION

Reactive oxygen species (ROS) like superoxide have been linked to pancreatic cancer. Superoxide is generated during normal aerobic metabolism and increased levels of these species are produced during various forms of oxidative stress. The net intracellular concentration of superoxide is the result of the production and the ability of antioxidants to remove it. MacMillan-Crow and colleagues have demonstrated 21- to 97-fold increases in levels of nitrotyrosine, a footprint of the reactive nitrogen species peroxynitrite (formed by the reaction of superoxide and nitric oxide), in pancreatic cancer specimens compared to normal pancreas (25). Findings from our laboratory add to MacMillan-Crowe's studies by demonstrating that pancreatic cancer cell lines have increased intracellular superoxide levels compared to other cell lines studied as measured by hydroethidine fluorescence (26). One reason why pancreatic cancer is so aggressive and unresponsive to treatments is its resistance to apoptosis. Vaquero and colleagues have recently demonstrated that ROS are prosurvival, antiapoptotic factors in pancreatic cancer (27). Their study showed that growth factors stimulate ROS generation by activation of membrane nonmitochondrial NAD(P)H oxidase and that inhibiting ROS by different approaches stimulates apoptosis in pancreatic cancer cells. Thus the prosurvival effect of superoxide may be an important mechanism of pancreatic cancer cell resistance to therapy. Our current study demonstrates that Rac1 plays a role in growth of pancreatic adenocarcinoma via a superoxide-mediated mechanism. Previous studies from our laboratory have also implicated superoxide as a mitogenic signaling molecule in pancreatic cancer (24, 28). Scavenging of superoxide with manganese superoxide dismutase (24), copper/zinc superoxide dismutase (28), or extracellular superoxide dismutase (28) all have similar effects in decreasing superoxide levels and inhibiting *in vitro* growth.

In a lung cancer model of tumorigenesis, K-ras activation combined with Rac1 deletion caused a profound decrease in proliferation (29). As a downstream effector protein of Ras, Rac1 activity is also regulated by Ras. There is growing evidence for Rac1 regulation of ROS in non-phagocytic cells. For example, stimuli that increase Rac1-GTP in gastric epithelial cells increase ROS production(30). Also, mutationally activated Rac1 induces ROS formation (31), and second site mutations showed that Rac1 activation ofROS production correlates with mitogenic stimulation, but not with actin polymerization or JNK activation (31).

Our findings demonstrate that Rac1 may be involved in the activation of NADPH oxidase leading to superoxide generation in some pancreatic cancer cells, it is still unclear about the specific structure of this enzyme complex. Recently, Nox (nonphagocytic NAD(P)H oxidase) proteins, homologous to gp91phox, have been identified in a variety of cell types, including pancreatic cancer cells (32, 33). Vaquero *et al.*, showed that different Nox isoforms are expressed in various pancreatic cancer cells, for example, Nox3 and Nox4 are expressed in MIAPaCa-2 cells, while Nox4 is expressed in Panc-1 cells (27). However, the modulation of Rac1 and the subsequent changes in superoxide and ROS generation through the NADPH oxidase pathway has remained uncharacterized in pancreatic cells.

In summary, in pancreatic cancer cells with mutant K-*ras*, a dominant/negative rac adenoviral construct decreased rac activity, decreased superoxide levels, and inhibited *in vitro* growth but had no effect in pancreatic cancer cells with wild-type K-*ras*.. Additionally, the same construct had no effect on an immortalized pancreatic ductal epithelial cell line, but decreased superoxide levels and inhibited *in vitro* growth in the isogeneic tumorigenic cell line that expresses K-*ras*. In addition, the Ad*N17Rac* construct inhibited *in vivo* tumor growth. These results suggest that activation of Rac1-dependent superoxide generation leads to pancreatic cancer cell proliferation. In pancreatic cancer inhibition of Rac1 may be a potential therapeutic target.

Supplementary Material

Refer to Web version on PubMed Central for supplementary material.

Acknowledgments

Supported by NIH grants CA115785, CA66081, the Susan L. Bader Foundation of Hope, and a Merit Review grant from the Medical Research Service, Department of Veterans Affairs

References

1. Uemura T, Hibi K, Kaneko T, Takeda S, Inoue S, Okochi O, et al. Detection of K-ras mutations in the plasma DNA of pancreatic cancer patients. J Gastroenterol. 2004; 39:56–60. [PubMed: 14767735]
2. Maisonneuve P, Lowenfels AB. Chronic pancreatitis and pancreatic cancer. Dig Dis. 2002; 20:32–37. [PubMed: 12145418]
3. Matallanas D, Arozarena I, Berciano MT, Aaronson DS, Pellicer A, Lafarga M, et al. Differences on the inhibitory specificities of H-Ras, K-Ras, and N-Ras (N17) dominant negative mutants are related to their membrane microlocalization. J Biol Chem. 2003; 278:4572–4581. [PubMed: 12458225]

4. Milasincic DJ, Calera MR, Farmer SR, Pilch PF. Stimulation of C2C12 myoblast growth by basic fibroblast growth factor and insulin-like growth factor 1 can occur via mitogen activated protein kinase-dependent and -independent pathways. Mol Cell Biol. 1996; 16:5964–5973. [PubMed: 8887626]

5. Crnogorac-Jurcevic T, Efthimiou E, Capelli P, Blaveri E, Baron A, Terris B, et al. Gene expression profiles of pancreatic cancer and stromal desmoplasia. Oncogene. 2001; 20:7437–7446. [PubMed: 11704875]

6. Bokoch GM, Diebold BA. Curent molecular models for NADPH oxidase regulation by Rac GTPase. Blood. 2002; 100:2692–2696. [PubMed: 12351373]

7. Didsbury J, Weber RF, Bokoch GM, Evans T, Snyderman R. Rac, a novel ras-related family of proteins that are botulinum toxin substrates. J Biol Chem. 1989; 264:16378–16382. [PubMed: 2674130]

8. Chan AY, Coniglio SJ, Chuang YY, Michaelson D, Knaus UG, Philips MR, et al. Roles of the Rac1 and Rac3 GTPases in human tumor cell invasion. Oncogene. 2005; 24:7821–7829. [PubMed: 16027728]

9. Gregg D, Rauscher FM, Goldschmidt-Clermont PJ. Rac regulates cardiovascular superoxide through diverse molecular interactions: more than a binary GTP switch. Am J Physiol, Cell Physiol. 2003; 285:723–734.

10. Sahai E, Marshall CJ. RHO-GTPases and cancer. Nat Rev Cancer. 2002; 2:133–142. [PubMed: 12635176]

11. Hordijk PL. Regulation of NADPH oxidases: the role of Rac proteins. Circ Res. 2006; 98:453–462. [PubMed: 16514078]

12. Irani K, Xia Y, Zweier JL, Sollott SJ, Der CJ, Fearon ER, et al. Mitogenic signaling mediated by oxidants in Ras-transformed fibroblasts. Science. 1997; 275:1649–1652. [PubMed: 9054359]

13. Sundaresan M, Yu ZX, Ferrans VJ, Sulciner DJ, Gutkind JS, Irani K, et al. Regulation of reactive-oxygen-species generation in fibroblasts by Rac1. Biochem J. 1996; 318:379–382. [PubMed: 8809022]

14. Moldovan L, Irani K, Moldovan NI, Finkel T, Goldschmidt-Clermont PJ. The actin cytoskeleton reorganization induced by Rac1 requires the production of superoxide. Antioxid Redox Signal. 1999; 1:29–43. [PubMed: 11225730]

15. Wetering S, Buul JD, Quik S, Mul FP, Anthony EC, Klooster JP, et al. Reactive oxygen species mediate Rac-induced loss of cell–cell adhesion in primary human endothelial cells. J Cell Sci. 2002; 115:1837–1846. [PubMed: 11956315]

16. Sulciner DJ, Irani K, Yu ZX, Ferrans VJ, Goldschmidt-Clermont P, Finkel T. Rac1 regulates a cytokine-stimulated, redox-dependent pathway necessary for NF-kappaB activation. Mol Cell Biol. 1996; 16:7115–7121. [PubMed: 8943367]

17. Zimmerman MC, Dunlay RP, Lazartigues E, Zhang Y, Sharma RV, Engelhardt JF, et al. Requirement for Rac1-dependent NADPH oxidase in the cardiovascular and dipsogenic actions of angiotensin II in the brain. Circ Res. 2004; 95:532–539. [PubMed: 15271858]

18. Yeh LH, Park YJ, Hansalia RJ, Ahmed IS, Deshpande SS, Goldschmidt-Clermont PJ, et al. Shear-induced tyrosine phosphorylation in endothelial cells requires Rac-1-dependent production of ROS. Am J Physiol. 1999; 276:C838–C847. [PubMed: 10199814]

19. Deem TL, Cook-Mills JM. Vascular cell adhesion molecule 1 (VCAM-1) activation of endothelial cell matrix metalloproteinases: role of reactive oxygen species. Blood. 2004; 104:2385–2393. [PubMed: 15265790]

20. Binker MG, Binker-Cosen AA, Richards D, Oliver B, Cosen-Binker LI. EGF promotes invasion by PANC-1 cells through Rac1/ROS-dependent secretion and activation of MMP-2. Biochem Biophys Res Commun. 2009; 379:445–450. [PubMed: 19116140]

21. Qian J, Niu J, Li M, Chiao PJ, Tsao MS. In vitro modeling of human pancreatic duct epithelial cell transformation defines gene expression changes induced by K-ras oncogenic activation in pancreatic carcinogenesis. Cancer Res. 2005; 65:5045–5053. [PubMed: 15958547]

22. Lewis A, Ough M, Du J, Tsao MS, Oberley LW, Cullen JJ. Targeting NAD(P)H:quinone oxidoreductase (NQO1) in pancreatic cancer. Molecular Carcinogenesis. 2005; 43:215–224. [PubMed: 16003741]

23. Jessop NW, Hay RJ. Preparation, preservation, recovery and use of irradiated feeder layers in cell culture research. TCA Manual. 1979; 5:1137–1139.
24. Wydert C, Roling B, Liu J, Ritchie JM, Oberley LW, Cullen JJ. Suppression of the malignant phenotype in human pancreatic cancer cells by the overexpression of manganese superoxide dismutase. Mol Cancer Ther. 2003; 2:361–369. [PubMed: 12700280]
25. MacMillan-Crow LA, Greendorfer JS, Vickers SM, Thompson JA. Tyrosine nitration of c-SRC tyrosine kinase in human pancreatic ductal adenocarcinoma. Arch Biochem Biophys. 2000; 377:350–356. [PubMed: 10845713]
26. Grady M, Gaut AW, Liu J, Zhang YP, Zhang HJ, Weydert C, et al. K-ras mutations in pancreatic cancer. Free Radic Biol Med. 2002; 33:S440.
27. Vaquero EC, Edderkaoui M, Pandol SJ, Gukovsky I, Gukovskaya AS. Reactive oxygen species produced by NAD(P)H oxidase inhibit apoptosis in pancreatic cancer cells. J Biol Chem. 2004; 279:34643–34654. [PubMed: 15155719]
28. Teoh MLT, Sun W, Smith BJ, Oberley LW, Cullen JJ. Modulation of reactive oxygen species (ROS) in pancreatic cancer: Insight into tumor growth suppression by the superoxide dismutases. Clin Cancer Res. 2007; 13:7441–7450. [PubMed: 18094428]
29. Kissil JL, Walmsley MJ, Hanlon L, Haigis KM, Kim CF, Sweet-Cordero A, et al. Requirement for Rac1 in a K-ras-induced lung cancer in a mouse. Cancer Res. 2007; 67:8089–8094. [PubMed: 17804720]
30. Kawahara T, Kiohjima M, Kuwano Y, Mino H, Teshima-Kondo S, Takeya R, et al. Helicobacter pylori lipopolysaccharide activates Rac1 and transcription of NADPH oxidase Nox1 and its organizer NOXO1 in guinea pig gastric mucosal cells. Am J Physiol. 2005; 288:C450–C457.
31. Joneson T, Bar-Sagi D. A Rac1 effector site controlling mitogenesis through superoxide production. J Biol Chem. 1998; 273:17991–17994. [PubMed: 9660749]
32. Wang S, Pogue R, Morre DM, Morre DJ. NADH oxidase activity (NOX) and enlargement of HeLa cells oscillate with two different temperature-compensated period lengths of 22 and 24 minutes corresponding to different NOX forms. Biochim Biophys Acta. 2001; 1539:192–204. [PubMed: 11420117]
33. Lim SD, Sun C, Lambeth JD, Marshall F, Amin M, Chung L, et al. Increased Nox1 and hydrogen peroxide in prostate cancer. Prostate. 2005; 62:200–207. [PubMed: 15389790]

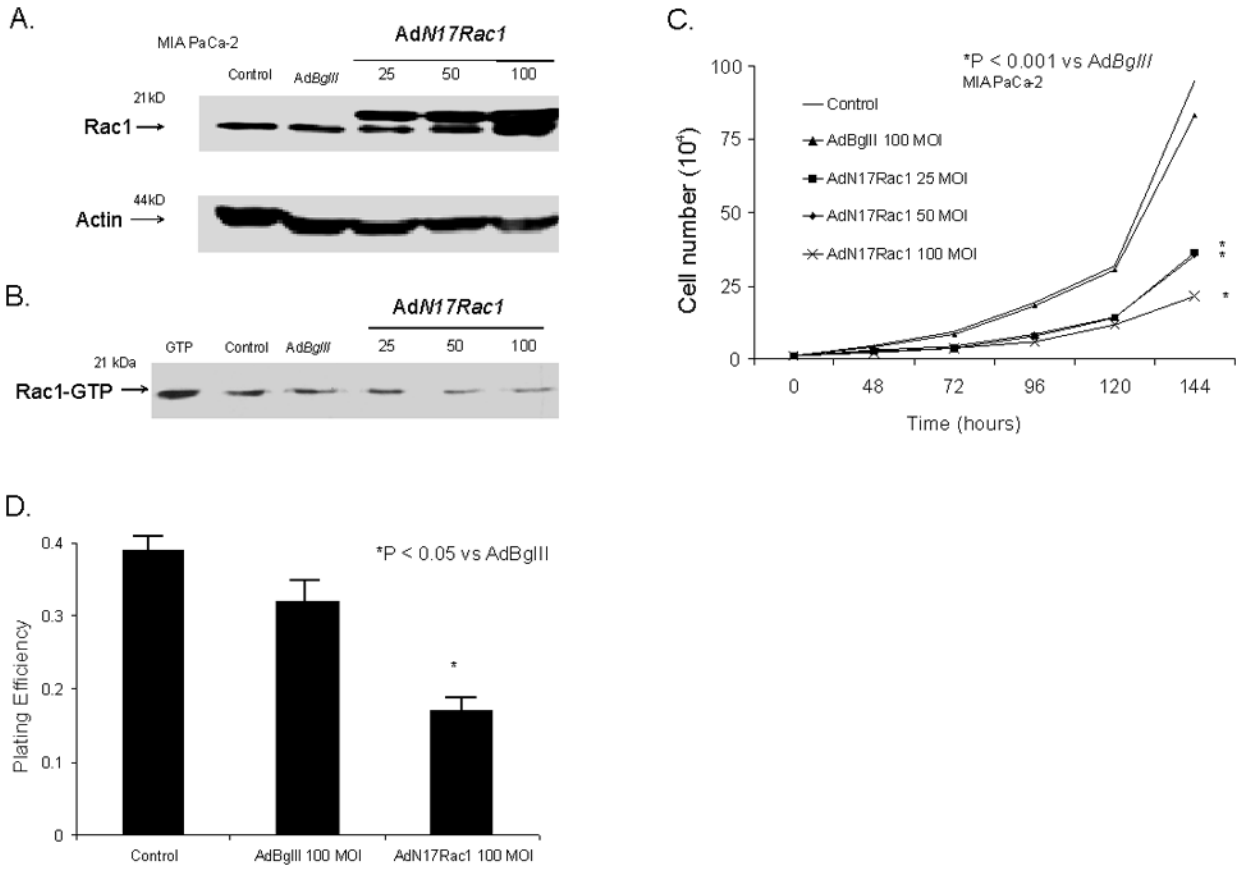

Figure 1.

Ad*Rac1N17* infection increased Rac1 protein levels, decreased Rac activity, and inhibited growth in MIAPaCa-2 cells. A. Cells transduced with 0-100 MOI Ad*Rac1N17* demonstrated increases in Rac1 immunoreactivity with increasing viral titer. No difference was seen with Ad*BglII* transfection compared with parental cells. For total Rac1 measurement, 30 μg cellular protein per well was used for western. All of the western blots were repeated to confirm the findings.

B. Representative western blot showing dose-dependent decreases in Rac1 activation in Ad*Rac1N17*-transduced MIAPaCa-2 cells. Ad*BglII* served as a control. Cell lysates were immunoprecipitated with PAK-1 PBD-agarose. Associated GTP-bound Rac1 was determined by immunoblotting with anti-Rac1 antibody. 10 nM GTP was added to untreated cells as the positive control.

C. Overexpression of Ad*Rac1N17* delayed MIAPaCa-2 cell growth. MIAPaCa-2 cells transduced with 0 100MOI Ad*Rac1N17* or 100 MOI Ad*BglII* demonstrated reductions in cell growth with Ad*Rac1N17*100 MOI. No significant changes were seen with Ad*BglII* transduction compared with parental cells. Mean *in vitro* cell growth of control, Ad*Rac1N17*-or Ad*BglII*-transduced MIAPaCa-2 cells are shown. Each point represents the mean values, $n = 3$. *P < 0.05 vs. 100 MOI Ad*BglII*.

D. Plating efficiency was decreased with increased Ad*Rac1N17* transduction in MIAPaCa-2 cells. MIAPaCa-2 cells were seeded at 5×10^5 cells / plate overnight until attached, transduced by Ad*Rac1N17* or Ad*BglII* for 24 hours, recovered in full media without

adenovirus for another 24 hours, and were then trypsinized and plated for clonogenic survival. Ad*Rac1N17* transduced cells decreased plating efficiency at 100 MOI. No significant changes were seen with Ad*BglII* transfer compared with parental cells. Each point represents the mean values, $n = 3$. *$P < 0.05$ vs.100 MOI Ad*BglII*.

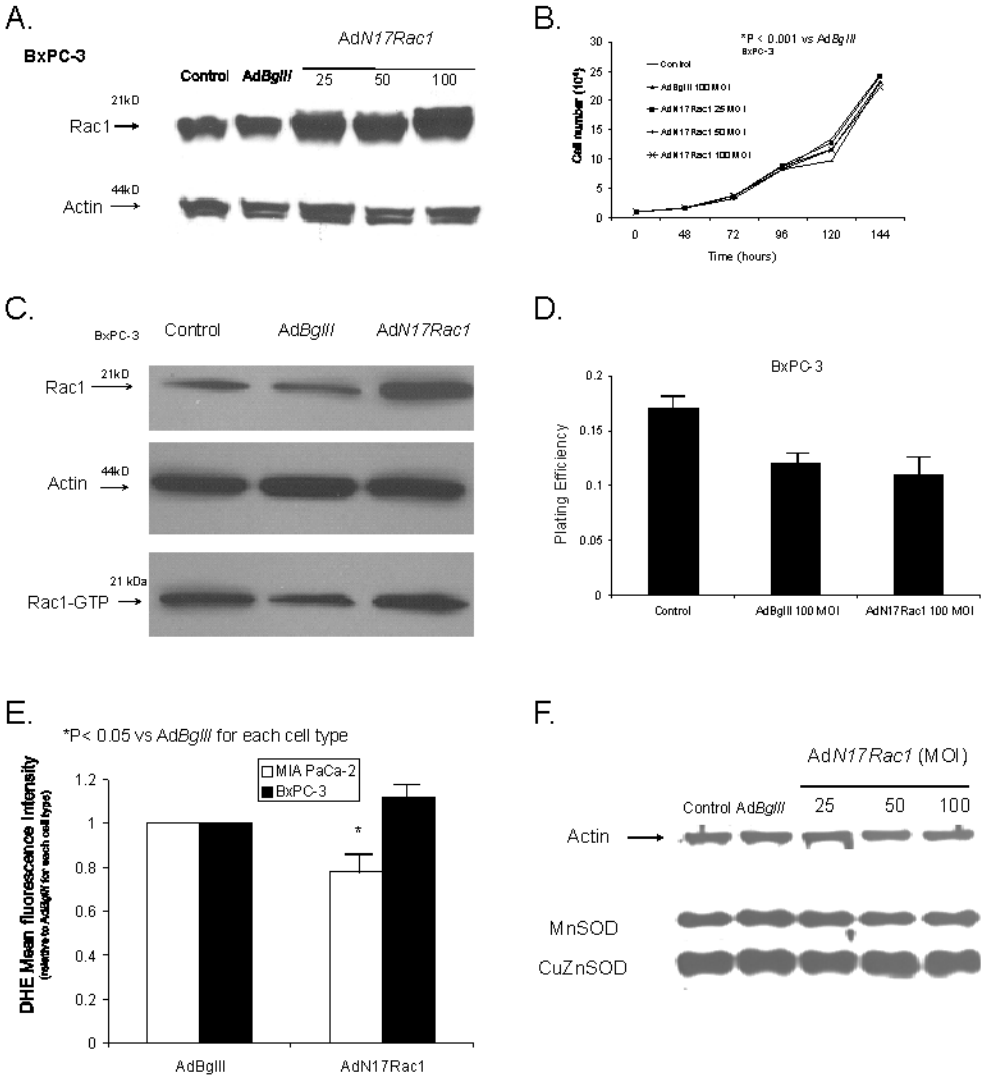

Figure 2.

Ad*Rac1N17* infection increased Rac1 protein levels but had no effect on growth in BxPC-3 cells. A. Cells transduced with 0–100 MOI Ad*Rac1N17* demonstrated increases in Rac1 immunoreactivity with increasing viral titer. No difference was seen with Ad*BglII* transfer compared with parental cells.

B. Overexpression of Ad*Rac1N17* had no effect on BxPC-3 cell growth. BxPC-3 cells transduced with 0 100MOI Ad*Rac1N17* or 100 MOI Ad*BglII* demonstrated no changes in cell growth with Ad*Rac1N17*100 MOI. No significant changes were seen with Ad*BglII* transduction compared with parental cells. Mean *in vitro* cell growth of control, Ad*Rac1N17*-or Ad*BglII*-transduced BxPC-3 cells are shown. Each point represents the mean values, $n = 3$. *P < 0.05 vs. 100 MOI Ad*BglII*.

C. Infection with Ad*Rac1N1* increased Rac1 immunoreactivity but did not decrease Rac1 activation in Ad*Rac1N17*-transduced BxPC-3 cells.

D. Plating efficiency was unchanged with Ad*Rac1N17* infection in BxPC-3 cells. BxPC-3 cells were infected with Ad*Rac1N17* or Ad*BglII* and then plated for clonogenic survival. Ad*Rac1N17* infected cells did not change plating efficiency at 100 MOI when compared to Ad*BglII* infected cells. Each point represents the mean values, $n = 3$.

E. Superoxide levels decreased in MIA PaCa-2 cells after infection with the Ad*N17Rac1* construct without changes in antioxidant proteins that scavenge superoxide. Intracellular hydroethidine fluorescence decreased in MIA PaCa-2 cells but not BxPC-3 cells infected with Ad*N17Rac1*. Intracellular superoxide levels as measured by DHE decreasedsignificantly 48 hours after infection with Ad*N17Rac1* 100 MOI compared to MIA PaCa-2 pancreatic carcinoma cells infected with the Ad*BglII* vector. *$p < 0.05$ vs Ad*BglII*, means ± SEM, n=3.

F. Overexpression of Ad*N17Rac1* did not change immunoreactive protein for MnSOD or CuZnSOD in MIA PaCa-2 cells. MIA PaCa-2 cells were transfected with 100 multiplicity of infection (MOI) of Ad*BglII* as a negative control or 0 to 100 MOI of Ad*N17Rac1*. After 48 hr of transfection, total cell lysate was prepared and immunoblotted for the proteins with cellular actin as a loading control. Total protein was electrophoresed in a 12.5% SDS-polyacrylamide running gel and a 5% stacking gel. After blocking in 20% fetal bovine serum for 1 hr, the sheets were washed and then treated with antibodies to MnSOD and CuZnSOD.

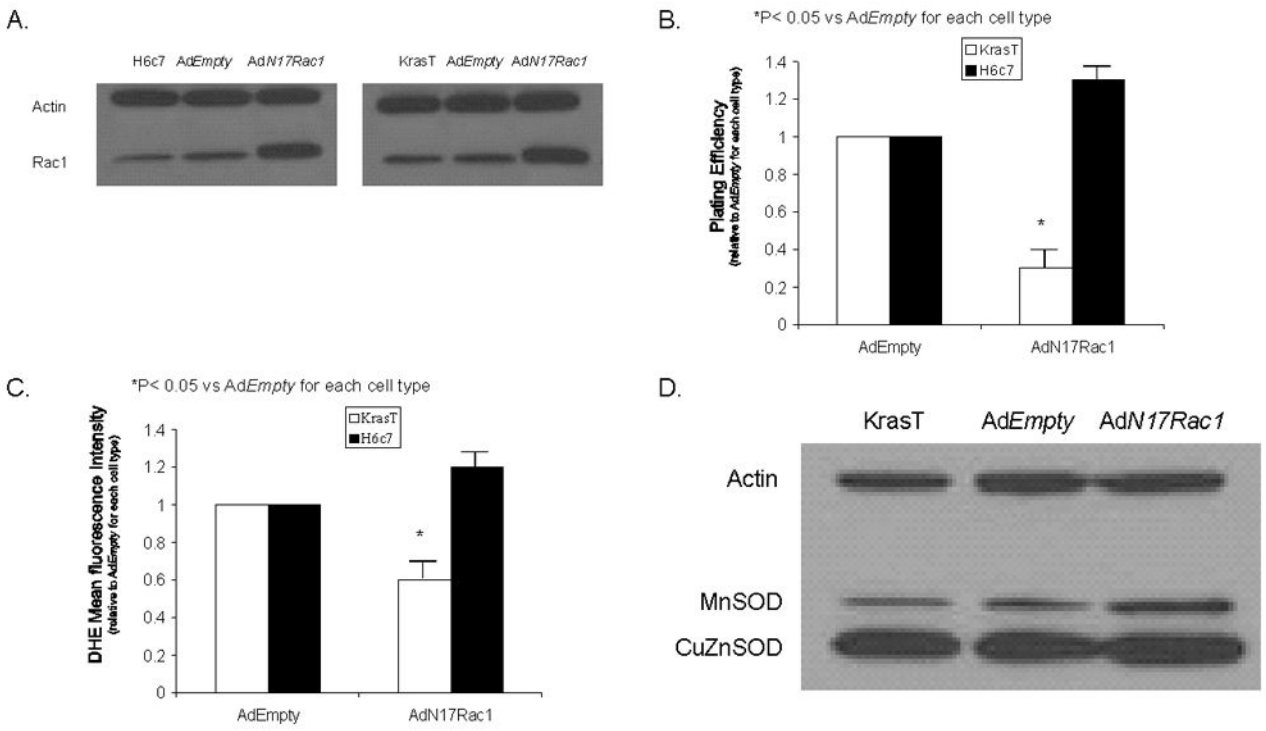

Figure 3.

Ad*Rac1N17* infection increases Rac1 protein levels, inhibits growth, and decreases superoxide levels in tumorigenic pancreatic ductal epithelial cells that express K-*ras*.

A. Cells transduced with 100 MOI Ad*Rac1N17* demonstrated increases in Rac1 immunoreactivity with increasing viral titer. No difference was seen with Ad*Empty* 100 MOI transfection compared with parental cells.

B. Plating efficiency was unchanged with Ad*Rac1N17* infection in H6c7 cells but decreased in KrasT cells. Feeder cells were used by irradiating B1 mouse fibroblasts Twenty-four hours before clonogenic assay, irradiated cells were thawed and diluted in keratinocyte serum free media. Cells were then seeded 3×10^5/ plate overnight until attached, transduced by Ad*Rac1N17* or Ad*Empty* for 24 hours, recovered in full media without adenovirus for another 24 hours, and then trypsinized and plated for clonogenic survival. No significant changes were seen plating efficiency in H6c7 cells infected with the Ad*Rac1N17mpty* vector. However, KrasT cells infected with Ad*Rac1N17* decreased plating efficiency. Each point represents the mean values, $n = 3$. $^*P < 0.05$ vs.100 MOI Ad*Empty*.

C. Superoxide levels decreased in KrasT cells after infection with the Ad*N17Rac1* construct. Intracellular hydroethidine fluorescence decreased in KrasT cells but not in H6c7 cells infected with Ad*N17Rac1*. Intracellular superoxide levels as measured by DHE decreased significantly 48 hours after infection with Ad*N17Rac1* 100 MOI compared to KrasT cells infected with the Ad*Empty* vector. *p < 0.05 vs Ad*empty*, means ± SEM, n=3.

D. Overexpression of Ad*N17Rac1* did not change immunoreactive protein for MnSOD or CuZnSOD in KrasT cells. KrasT cells were transfected with 100 multiplicity of infection (MOI) of Ad*Empty* as a negative control or 100 MOI of Ad*N17Rac1*. After 48 hr of transfection, total cell lysate was prepared and immunoblotted for MnSOD and CuZnSOD.

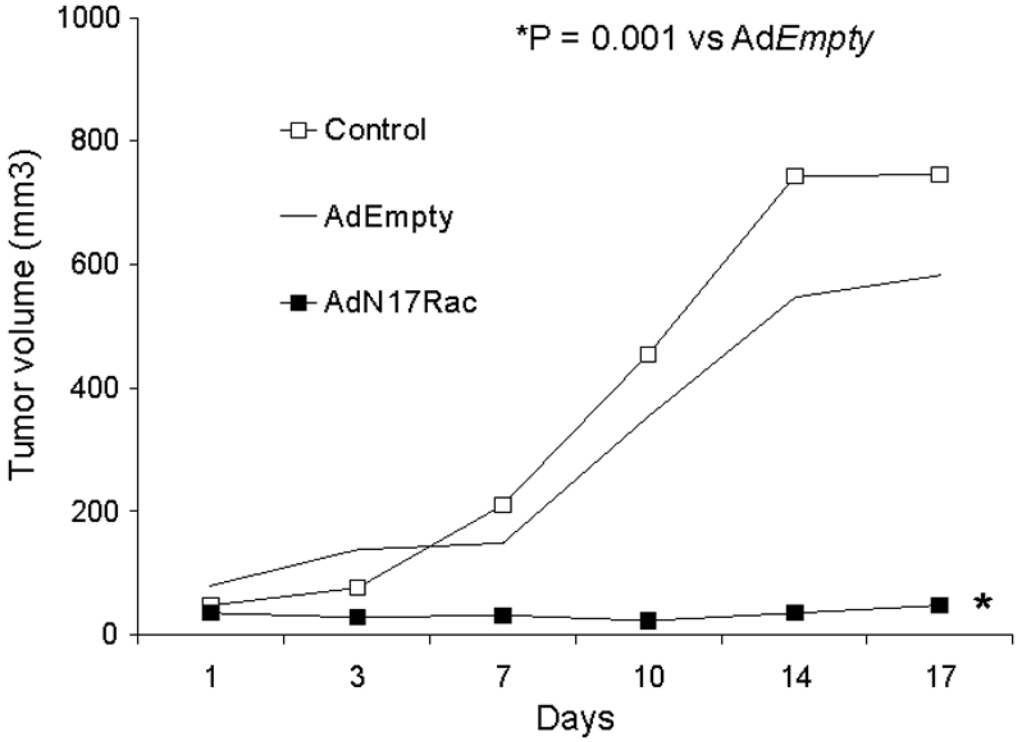

Figure 4.

Ad*N17Rac1* injections decreased MIA PaCa-2 tumor growth in nude mice. The Ad*N17Rac1*group had significantly slower tumor growth when compared to the control and Ad*Empty*, ($p < 0.001$, n = 7–8/group). MIA PaCa-2 tumor cells (3×10^6) were delivered subcutaneously into the flank region of nude mice. Controls received serum-free media in similar volumes. 1×10^9 PFUs of the Ad*N17Rac1* or Ad*Empty* constructs were delivered to the tumor on day 1, 7, and 14 of the experiment. On day 17 there was a 10-fold decrease in tumor growth in animals receiving the Ad*N17Rac1* vector when compared to treatment with the Ad*Empty* control vector.